Available online at www.sciencedirect.com

SCIENCE DIRECT®

Solar Energy 77 (2004) 137–157

SOLAR ENERGY

www.elsevier.com/locate/solener

# Models of sky radiance distribution and sky luminance distribution

Norio Igawa [a,*], Yasuko Koga [b], Tomoko Matsuzawa [c], Hiroshi Nakamura [d]

[a] *Research and Development Institute, Takenaka Corporation, 1-5-1, Ohtsuka, Inzai, Chiba 270-1395, Japan*
[b] *Kyushu University, 6-10-1, Hakozaki, Higashi-ku, Fukuoka 812-8581, Japan*
[c] *Kyushu Kyoritsu University, 1-8, Jiyugaoka, Yahatanishi-ku, Kitakyushu 807-8585, Japan*
[d] *Kyushu University, 6-203, Town-Kamiyagoto, Hachimanyama, Tempaku-ku, Nagoya 468-0074, Japan*

Received 22 July 2003; received in revised form 28 April 2004; accepted 29 April 2004
Available online 19 June 2004

Communicated by: Associate Editor David Renne

**Abstract**

The aim of this research work is to propose sky radiance and luminance distribution models for all sky conditions from clear sky to overcast sky. The classification method of sky conditions is examined. Clear sky index is defined based on the global irradiance. Cloudless index is defined based on the global irradiance and the diffuse irradiance. The sky conditions are classified according to both indices. The data of the average sky radiance (luminance) distributions are obtained based on the classified sky conditions. The average relative sky radiance distributions are compared with the average relative sky luminance distributions. It has been confirmed that both radiance/luminance distributions can be shown by the same equation.

An equation that shows the relative sky radiance (luminance) distribution for all sky conditions and equations that show the zenith radiance and the zenith luminance are obtained. The absolute value of the sky radiance (luminance) distribution is shown by multiplying the relative sky radiance (luminance) distribution and the zenith radiance (luminance). The equations to show the absolute values of the sky radiance distribution called the All Sky Model-R and the sky luminance distribution called the All Sky Model-L are proposed.

Both models are compared with the previous models based on the measurement distributions concerning the region of sky vault and the sky conditions and good results are obtained. In addition, the vertical irradiance and illuminance calculated by the proposed models and the previous models are compared with the measurements, and the proposed models are confirmed their accuracy.


*Keywords:* Sky radiance distribution; Sky luminance distribution; Modeling

## 1. Introduction

The meteorological data that can reproduce the weather condition as accurately as possible is necessary for the effective use of solar energy and the plan and design of energy conservation in buildings. Data concerning the solar radiation and daylight are the most basic meteorological data. It is necessary to establish the overall design technique for the thermal and luminous environment to implement energy conservation and to ensure the quality of the indoor environment. For this purpose, detailed, realistic models for the solar radiation and the daylight are indispensable. Till today, there are a lot of considerations about modeling sky radiance and luminance distributions. However, most of models do

* Corresponding author. Tel.: +81-476-47-1700; fax: +81-476-46-6688/+81-476-47-3080.
*E-mail address:* igawa.norio@takenaka.co.jp (N. Igawa).

0038-092X/$ - see front matter © 2004 Elsevier Ltd. All rights reserved.
doi:10.1016/j.solener.2004.04.016

**Nomenclature**

| | |
|---|---|
| $A$ | coefficient for the zenith radiance (luminance) |
| $a$ | coefficient for the gradation function |
| $B$ | coefficient for the zenith radiance (luminance) |
| $b$ | coefficient for the gradation function |
| $C$ | coefficient for the zenith radiance (luminance) |
| $c$ | coefficient for the scattering indicatrix function |
| Ce | cloud ratio |
| $\mathrm{Ce_s}$ | standard cloud ratio |
| Cle | cloudless index |
| $d$ | coefficient for the scattering indicatrix function |
| $e$ | coefficient for the scattering indicatrix function |
| Eed | diffuse irradiance ($W/m^2$) |
| Eeg | global irradiance ($W/m^2$) |
| $\mathrm{Eeg^{cl}}$ | global irradiance of clear sky ($W/m^2$) |
| Eeo | extraterrestrial direct normal irradiance ($W/m^2$) |
| Evd | diffuse illuminance (lx) |
| $f(\zeta)$ | scattering indicatrix function |
| Kc | clear sky index |
| $\mathrm{Lcl}(\gamma_s, \gamma, \zeta)$ | equivalent luminance of the sky element of CIE Standard Clear Sky |
| $\mathrm{LclR}(\gamma_s, \gamma, \zeta)$ | relative luminance of the sky element of CIE Standard Clear Sky |
| $\mathrm{Le}(\gamma_s, \gamma, \zeta)$ | relative sky radiance distribution |
| $\mathrm{Lea}(\gamma_s, \gamma, \zeta)$ | sky radiance distribution ($W/m^2$ sr) |
| $\mathrm{Lez}(\gamma_s)$ | zenith radiance ($W/m^2$ sr) |
| $\mathrm{Lv}(\gamma_s, \gamma, \zeta)$ | relative sky luminance distribution |
| $\mathrm{Lva}(\gamma_s, \gamma, \zeta)$ | sky luminance distribution ($cd/m^2$) |
| $\mathrm{Lvz}(\gamma_s)$ | zenith luminance ($cd/m^2$) |
| $\mathrm{Lzcl}(\gamma_s)$ | equivalent zenith luminance of CIE Standard Clear Sky |
| LzEd | inverse of the integration value of the relative sky radiance (luminance) distribution |
| $m$ | relative optical air mass |
| MBE | mean bias error |
| RMSE | root mean square error |
| Seeg | standard global irradiance ($W/m^2$) |
| Si | sky index |
| TL | Linke's turbidity factor |

*Greek symbols*

| | |
|---|---|
| $\alpha$ | azimuth angle of the sky element (rad) |
| $\alpha_s$ | azimuth angle of the sun (rad) |
| $\gamma$ | altitude of the sky element (rad) |
| $\gamma_s$ | solar altitude (rad) |
| $\gamma_{sz}$ | zenith angle of the sun (deg) |
| $\zeta$ | angular distance between the sun and the sky element (rad) |
| $\eta_d$ | diffuse luminous efficacy (lm/W) |
| $\phi(\gamma)$ | gradation function |

not explain continuously all sky conditions which fluctuate from clear sky to overcast sky.

Harrison and Coombes (1988) and Harrison (1991) proposed the sky radiance distribution model and the sky luminance distribution model as a function of the opaque cloud cover. Brunger and Hooper (1993) proposed an equation of the sky radiance distribution from clear sky to overcast sky as functions of the cloud ratio, and the atmospheric clearness index. Grant et al. (1996) proposed sky radiance distribution models of UVA (320–400 nm), UVB (280–320 nm), and PAR (400–700 nm). Nakamura et al. (1997a,b,c) proposed a sky radiance distribution model of the average sky based on the measurement data of IDMP (International Daylighting Measurement Programme) of CIE (Commission Internationale de l'Éclairage) in Fukuoka. Nagata (1997) proposed a numerical equation of sky radiance distribution of overcast sky based on the measurement data in Fukui.

Moon and Spencer (1942) surveyed and arranged previous research works, and proposed a luminance distribution model of overcast sky. This overcast sky model was simplified a little, and has been recommended as the CIE Standard Overcast Sky by CIE (1955). Kittler (1967) proposed a luminance distribution model of clear sky. This clear sky model has been recommended as the CIE Standard Clear Sky (CIE, 1973). Littlefair (1981) proposed an average sky luminance distribution model called the BRE Average Sky. Nakamura et al. (1985, 1987) proposed the Intermediate Sky and an equation of zenith luminance. Kittler (1985) proposed the Homogeneous Sky to show absolute values of sky luminance distribution. Perraudeau (1988) classified all the skies into five categories and proposed an equation of sky luminance distribution. Perez et al. (1993) proposed the All-weather Model as functions of Sky clearness and Sky brightness by which all skies were classified into eight categories. Kittler et al. (1997) classified all the sky conditions into 15 categories, and proposed the numerical equations to show these categorized sky luminance distributions. Afterwards, CIE (2003) recommended this model as the CIE Standard General Sky.

Authors (Matsuzawa et al., 1997; Igawa et al., 1997, 2002; Igawa and Nakamura, 2001) have proposed the sky luminance distribution model and the sky radiance distribution model where all sky conditions were continuously shown based on the measurement data of IDMP of CIE. This paper is the improvement and integration of these sky luminance and radiance distribution models.

## 2. Measurement of raw data

The raw data were gathered by the measurement conforming to the guide of IDMP of CIE (1994). The measurement data in Tokyo (35°40′N, 139°49′E) from March 1992 to September 1993 and in Fukuoka (33°31′N, 130°28′E) from January 1994 to December 1994 are used for this research work. The measuring instrument of the sky radiance and luminance distributions is the sky scanner developed by Nakamura et al. (1991). The angular aperture of the sensor for the radiance and luminance is 11°, and the half angle is 5.5°. The sky radiance and luminance distributions were measured every 15 min in Tokyo and every 30 min in Fukuoka from sunrise to sunset. The measurement points are 145 points on the sky vault. The sky radiance distribution was measured simultaneously with the sky luminance distribution. It took about three and a half minutes per measurement. The global horizontal, direct normal, diffuse horizontal and vertical (North, East, South, West) irradiances and illuminances are measured at one-minute interval. Matt black ground shields are attached to vertical irradiance and illuminance sensors forming an artificial horizon to screen ground-reflection. The perpendicular distance between the sensor and the end of the ground shield is more than 10 times the diameter of the cell. Upward reflection within the artificial horizon is minimized by using a matt black punched plate.

Because the solar radiation is attenuated by scattering and absorption the in atmosphere, the relative optical air mass produces a big influence on the surface irradiance. The Relative optical air mass can be expressed as a function of solar altitude. Thus, all the acquired data are sorted expediently by solar altitude in five-degree intervals. The values of the radiance and luminance at the symmetry positions to the sun meridian are averaged. The lowest altitude of sky elements measured for sky radiance is 6°. Because surrounding buildings influence data at the lowest altitude of sky elements, 30 acquired data at this altitude are excluded from the examination. And the data of sky elements of which angular distance between the sun are smaller than 15° are excluded from the regression analysis, because they are influenced by the direct solar beam. In this research work, the data are used for all cases when the solar altitude was higher than 5°.

## 3. Indices to classify sky conditions

A lot of indices are used to classify sky conditions for modeling sky radiance or luminance distributions. Perez et al. (1993) adopted the sky clearness and the sky brightness and Brunger and Hooper (1993) adopted the cloud ratio and the atmospheric clearness index for the classification of sky conditions. Here, the method of estimating sky conditions by the indices that can be easily obtained is examined. Generally, it is difficult to obtain the daylight data, though the solar radiation data can be obtained comparatively easily in various sites.

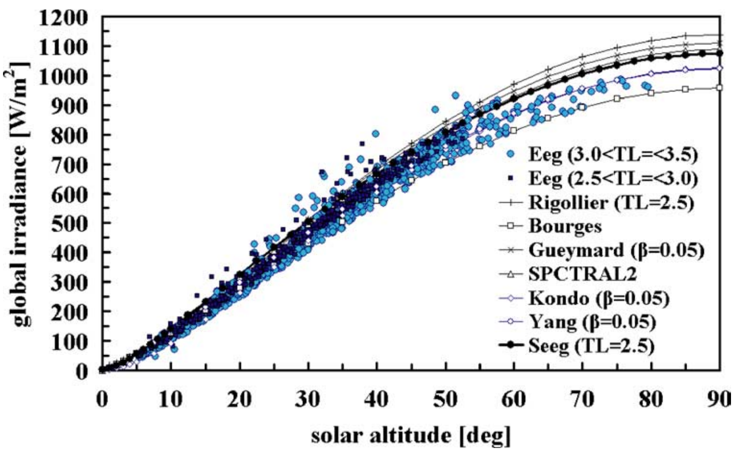


Fig. 1. The clear sky global irradiance measured of $2.5 < TL \leqslant 3.0$ and $3.0 < TL \leqslant 3.5$ and the clear sky global irradiance calculated and the standard global irradiance.

Therefore it is tried to classify sky conditions based on the solar radiation data.

The global irradiance is considered to be a useful index to classify sky conditions. However, the composition ratio of the direct irradiance and diffuse irradiance is not always the same for the global irradiance. It is appropriate to use the global irradiance together with the cloud ratio to classify sky conditions. However, the characteristics of the global irradiance and the cloud ratio depend on the solar altitude. The new indices without dependency on the solar altitude are examined based on the global irradiance and the cloud ratio.

### 3.1. Global irradiance and clear sky index

When the global irradiance is divided by the maximum value of the global irradiance at the same solar altitude, a new index without solar altitude dependency is obtained. Usually the maximum value of the global irradiance appears in the clear sky. Various models are proposed about the clear sky irradiance.

Bourges (1979) proposed a simple equation of the global irradiance. Kasten (1984) proposed the clear sky global irradiance by the Linke's turbidity factor and the relative optical air mass. Bird (1984) proposed the direct normal irradiance and the diffuse irradiance of the clear sky and afterwards the program SPCTRAL2 was presented. Gueymard (1989) proposed the equations to calculate the direct normal irradiance and the diffuse irradiance of the clear sky by Angstrom's turbidity coefficient etc. and afterwards the program SMARTS2 was presented. Rigollir et al. (2000) proposed the equations where the direct normal irradiance and the diffuse irradiance were shown by Linke's turbidity factor for European Solar Radiation Atlas. Kondo (2000) proposed a simple Basic program to calculate the clear sky global irradiance by Angstrom's turbidity coefficient and so on. Yang et al. (2001) proposed the equations to calculate the direct normal irradiance and the diffuse irradiance of clear sky by Angstrom's turbidity coefficient and so on.

Linke's turbidity factor of the daylight in the CIE Standard Clear Sky is assumed to be 2.45. The CIE Standard Clear Sky is applied with the considerable wide range of the turbidity factor. It is preferable that the turbidity factor of the clear sky is smaller than or equal to the turbidity factor of the CIE Standard Clear Sky. Though the turbidity factor of daylight and the turbidity factor of radiation is not the same, it is suitable to examine the global irradiance of which Linke's turbidity factor (TL) is about 2.5. Since various parameters are used in the above-mentioned equations, the parameter of each equation is set so that Linke's turbidity factor may become 2.5 equivalent. The global irradiance of the clear sky estimated by above-mentioned equations and the global irradiance by the measurement in the range of $2.5 < TL \leqslant 3.0$ and $3.0 < TL \leqslant 3.5$ is shown in Fig. 1. Each equation indicates a little different value respectively. These equations are compared with the

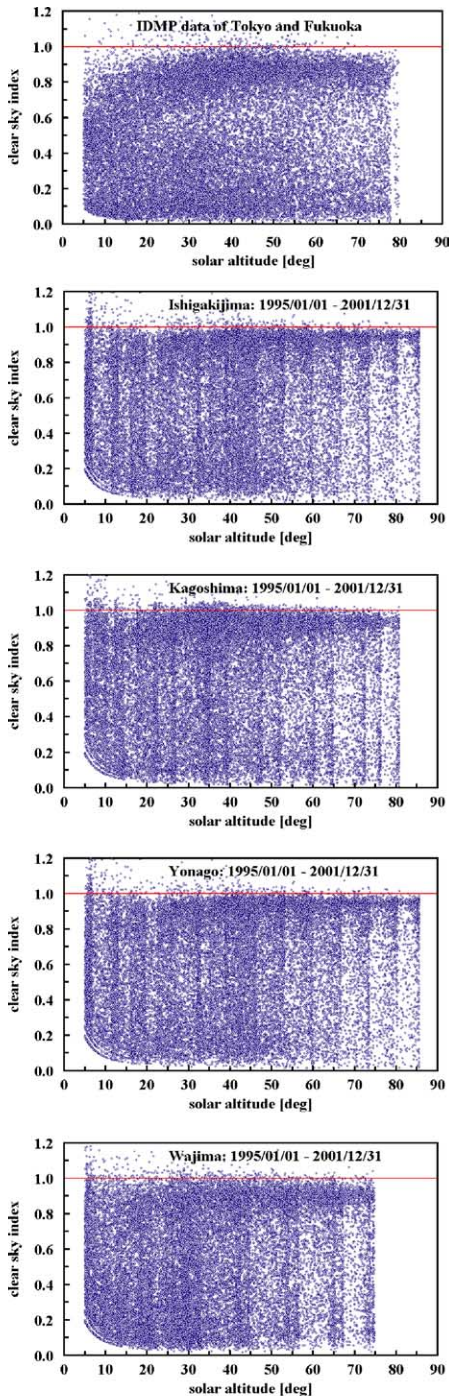


Fig. 2. The clear sky index at various sites.

measurement values, and the equation by Kasten is selected for its simplicity and arranged as follows:

$$\mathrm{Eeg_{cl}} = 0.84 \cdot \mathrm{Eeo}/m \cdot \exp(-0.027 \cdot \mathrm{TL} \cdot m) \quad (1)$$

where $\mathrm{Eeg_{cl}}$ is the global irradiance of clear sky (W/m$^2$), Eeo the extraterrestrial direct normal irradiance (1367 W/m$^2$), TL Linke's turbidity factor and $m$ the relative optical air mass (Kasten and Young, 1989).

The calculation value of Eq. (1) when TL = 2.5 is assumed to be the maximum global irradiance. The maximum global irradiance is almost equal to the measurement value of the global irradiance of TL = 2.5. Therefore, Eq. (1) with TL = 2.5 is defined as the standard global irradiance.

$$\mathrm{Seeg} = 0.84 \cdot \mathrm{Eeo}/m \cdot \exp(-0.0675 \cdot m) \quad (2)$$

where Seeg is the standard global irradiance (W/m$^2$), $m$ the relative optical air mass (Kasten and Young, 1989). The value of the global irradiance divided by the standard global irradiance is defined as the clear sky index.

$$\mathrm{Kc} = \frac{\mathrm{Eeg}}{\mathrm{Seeg}} \quad (3)$$

where Kc is the clear sky index.

The clear sky index calculated by Eq. (3) based on the measurement data of IDMP (Tokyo and Fukuoka) and the measurement data from 1995 to 2001 of the Japan Meteorological Agency, 1995-2001 in Ishigakijima (124°10′E, 24°20′N), Kagoshima (130°33′E, 31°33′N), Yonago (133°21′E, 35°26′N) and Wajima (136°54′E, 37°23′N) are shown in Fig. 2. Most of the clear sky indexes are laid from 1 to 0, that is, from clear sky to overcast sky. The clear sky index can be used as an index without dependency of the solar altitude to classify sky conditions.

### 3.2. Cloud ratio and cloudless index

Since the lower bound values of the cloud ratio appear in the clear sky and depend on the solar altitude, an index without solar altitude dependency is examined based on the cloud ratio. The diffuse irradiance divided by the global irradiance is defined as the cloud ratio

$$\mathrm{Ce} = \frac{\mathrm{Eed}}{\mathrm{Eeg}} \quad (4)$$

where Ce is the cloud ratio, Eed the diffuse irradiance (W/m$^2$) and Eeg the global irradiance (W/m$^2$).

Because Linke's turbidity factor of the standard global irradiance was indicated by 2.5, the cloud ratio of TL = 2.5 is obtained by the regression analysis based on the measurement cloud ratio data as the lower bound value and called the standard cloud ratio as follows:

$$\mathrm{Ce_s} = 0.01299 + 0.07698 \cdot m - 0.003857 \cdot m^2 + 0.0001054 \cdot m^3 - 0.000001031 \cdot m^4 \quad (5)$$

where $\mathrm{Ce_s}$ is the standard cloud ratio.

The cloud ratios measured of $2.5 < \mathrm{TL} \leqslant 3.0$ and $3.0 < \mathrm{TL} \leqslant 3.5$ and the cloud ratios calculated based on the above-mentioned clear sky irradiance models and the standard cloud ratio are shown in Fig. 3. The standard cloud ratio is almost equal to the minimum values of the cloud ratio measured and is near the mean value of the calculation values. The following value is defined as the cloudless index.

$$\mathrm{Cle} = \frac{1 - \mathrm{Ce}}{1 - \mathrm{Ce_s}} \quad (6)$$

where Cle is the cloudless index.

The cloudless index calculated by Eq. (6) based on the measurement data is shown in Fig. 4. The cloudless

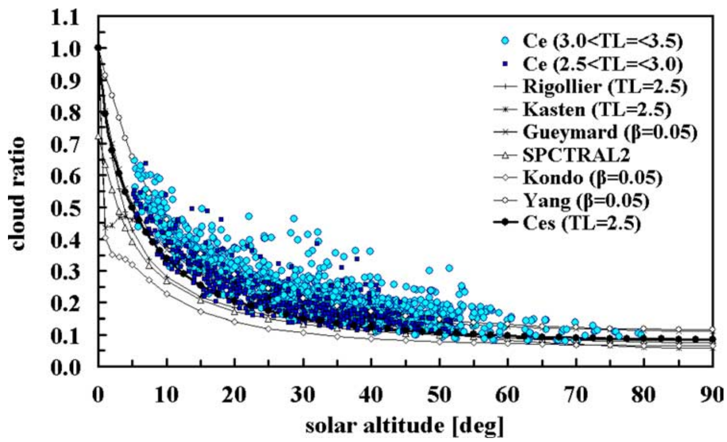


Fig. 3. The clear sky cloud ratio measured of $2.5 < \mathrm{TL} \leqslant 3.0$ and $3.0 < \mathrm{TL} \leqslant 3.5$ and the clear sky cloud ratio calculated and the standard cloud ratio.

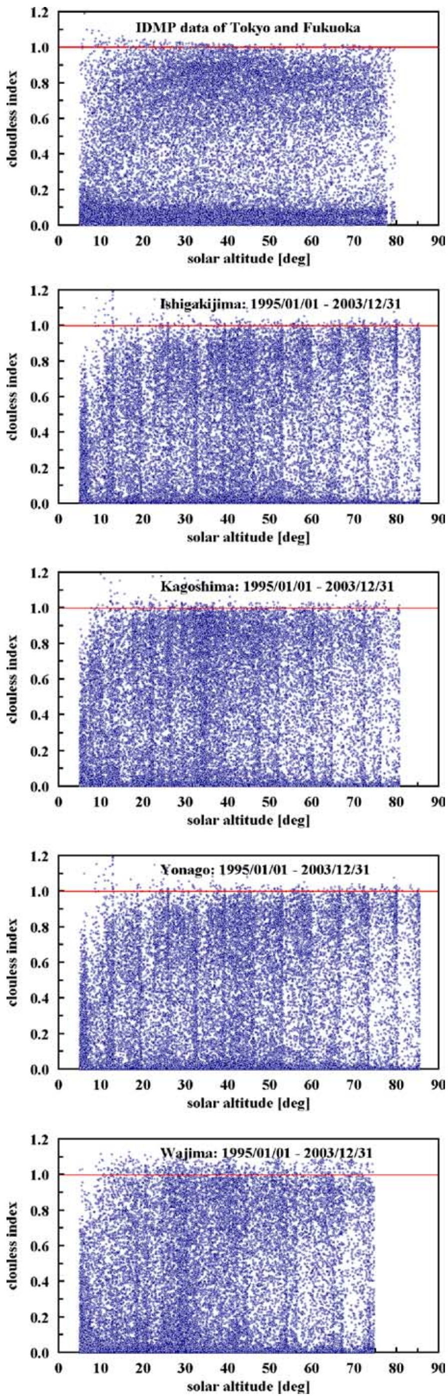


Fig. 4. The cloudless index at various sites.

indices of all the solar altitude are almost in the range from 1 to 0 though they vary a little when the solar altitude is low. The cloudless index proposed here can be used as the index without solar altitude dependency to classify sky conditions from clear sky to overcast sky.

### 3.3. Classification of sky conditions

The clear sky index and the cloudless index are suitable to classify the outline of sky conditions. In addition, the sky condition can be classified in detail by combining both indices like the matrix. Here, it is tried to classify all the sky conditions from clear sky to overcast sky, and to obtain the classified average sky radiance (luminance) distribution data as the following procedure.

(1) Data concerning the sky radiance distribution, the sky luminance distribution and the irradiances acquired by the measurement are arranged at solar altitude of 5° intervals.
(2) The clear sky index and the cloudless index are combined as the matrix, and all the sky conditions are classified by dividing both indices into every 0.1 intervals, respectively, in each solar altitude band.
(3) The measurement data of Tokyo and Fukuoka are classified according to the above-mentioned procedure.
(4) The average sky radiance (luminance) distributions for all the classified sky conditions are obtained at both sites, and these are assumed to be the basic sky radiance (luminance) distribution data for the formulation.
(5) The contour diagrams of the relative sky radiance distribution and the relative sky luminance distribution are obtained.

The coefficients of correlation between the relative sky radiance distributions and the relative sky luminance distributions in Tokyo and Fukuoka are shown in Fig. 5. Very high correlations are found between the relative sky radiance distributions and the relative sky luminance distributions in most sky conditions. The relative sky radiance distributions and the relative sky luminance distributions in Tokyo and Fukuoka are illustrated in Fig. 6. When the values of the clear sky index and the cloudless index increase, the sky condition indicates the tendency to change from overcast sky to clear sky. Because the differences between the relative sky radiance distributions and the relative sky luminance distributions are small, both are drawn quite similarly on the contour diagrams. Therefore, it is appropriate to show the relative sky radiance distribution and the relative sky luminance distribution by the same equation.

## 4. Formulation of sky radiance and luminance distributions

It is convenient that the sky radiance distribution and the sky luminance distribution can be shown

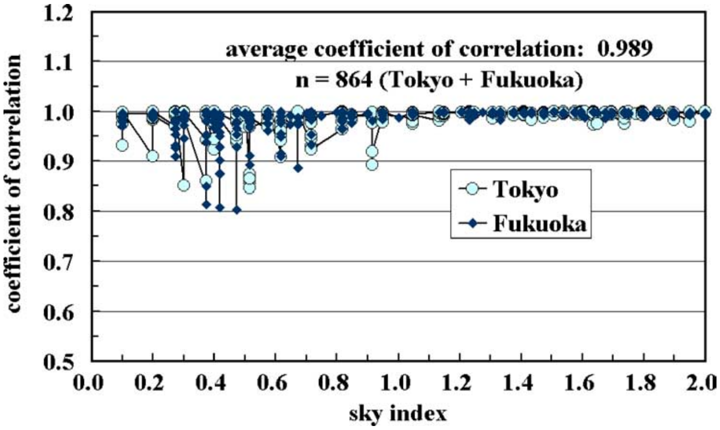


Fig. 5. The coefficients of correlation between the relative sky radiance distributions and the relative sky luminance distributions in Tokyo and Fukuoka. The sky index is defined as the sum of the clear sky index and the root of cloudless index.

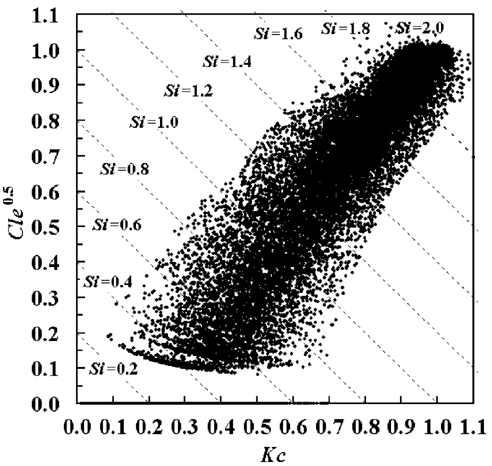


Fig. 6. An example of the relationship between the clear sky index and the root of cloudless index (Kagoshima 1995/1–2001/12).

continuously for all sky conditions. It is already confirmed that the sky radiance distribution of the clear sky and the overcast sky can be shown by the equations similar to the CIE Standard Clear Sky and the CIE Standard Overcast Sky, respectively. Therefore, referring to the equations of the sky luminance distribution, the basic equation to show the sky radiance distribution and the sky luminance distribution for all sky conditions is selected. All the coefficients of the equation are decided after the regression analysis based on the basic sky radiance distribution data for the formulation of Tokyo. After the equation of the relative sky radiance distribution is fixed, this equation is applied to the relative sky luminance distribution.

### 4.1. Formulation of sky radiance distribution

The sky luminance distribution of CIE Standard Clear Sky is shown as follows as the product of the scattering indicatrix function $f(\zeta)$ and the gradation function $\varphi(\gamma)$.

$$\mathrm{LclR}(\gamma_s,\gamma,\zeta) = \frac{\mathrm{Lcl}(\gamma_s,\gamma,\zeta)}{\mathrm{Lzcl}(\gamma_s)} = \frac{f(\zeta)\cdot\phi(\gamma)}{f(\pi/2-\gamma_s)\cdot\phi(\pi/2)} \quad (7)$$

where $\mathrm{LclR}(\gamma_s,\gamma,\zeta)$ is the relative luminance of the sky element of CIE Standard Clear Sky, $\mathrm{Lcl}(\gamma_s,\gamma,\zeta)$ the equivalent luminance of the sky element of CIE Standard Clear Sky, $\mathrm{Lzcl}(\gamma_s)$ the equivalent zenith luminance of CIE Standard Clear Sky, $f(\zeta) = 0.91 + 10\cdot\exp(-3\cdot\zeta) + 0.45\cdot\cos^2\zeta$ the scattering indicatrix function, $\phi(\gamma) = 1-\exp(-0.32/\sin\gamma)$ the gradation function, $\gamma_s$ the solar altitude (rad), $\gamma$ the altitude of the sky element (rad) and $\zeta$ the angular distance between the sun and the sky element (rad).

Following the CIE Standard Clear Sky, the basic equation of the relative sky radiance distribution for all sky conditions is decided as follows:

$$\mathrm{Le}(\gamma_s,\gamma,\zeta) = \frac{L(\gamma,\zeta)}{L(\pi/2,\pi/2-\gamma_s)} \quad (8)$$

where $\mathrm{Le}(\gamma_s,\gamma,\zeta)$ is the relative sky radiance of sky element, $L(\gamma,\zeta) = \phi(\gamma)\cdot f(\zeta)$ the equivalent radiance of sky element, $L(\pi/2,\pi/2-\gamma_s) = \phi(\pi/2)\cdot f(\pi/2-\gamma_s)$ the equivalent zenith radiance, $f(\zeta) = 1 + c\cdot\{\exp(d\cdot\zeta) - \exp(d\cdot\pi/2)\} + e\cdot\cos^2\zeta$ the scattering indicatrix function, $\phi(\gamma) = 1 + a\cdot\exp(b/\sin\gamma)$ the gradation function and $a$, $b$, $c$, $d$, $e$ the coefficients.

The altitudes of the sky elements measured concerning the sky radiance and luminance distribution are 6°, 18°, 30°, 42°, 54°, 66°, 78° and 90°. Because the

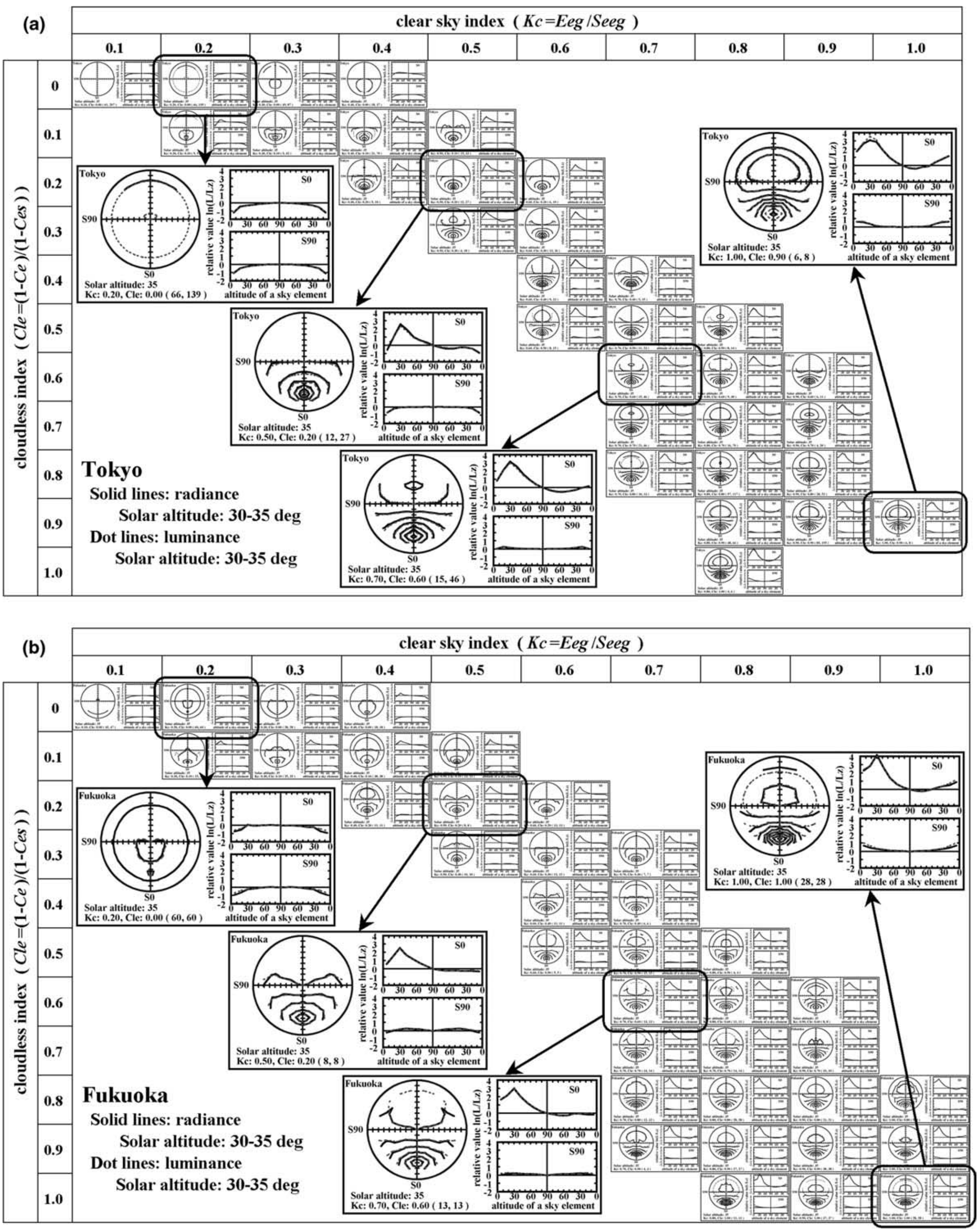


Fig. 7. The relative sky radiance distributions and the relative sky luminance distributions in Tokyo and Fukuoka.

measurement number of the sky elements at high altitude is few, the altitudes of the sky element from 18° to 54° are given priority for the regression analysis to fix the coefficients. Coefficients $a$, $b$, $c$, $d$, and $e$ are obtained by the regression analysis by Eq. (8) based on the basic sky radiance distribution data for the formulation of

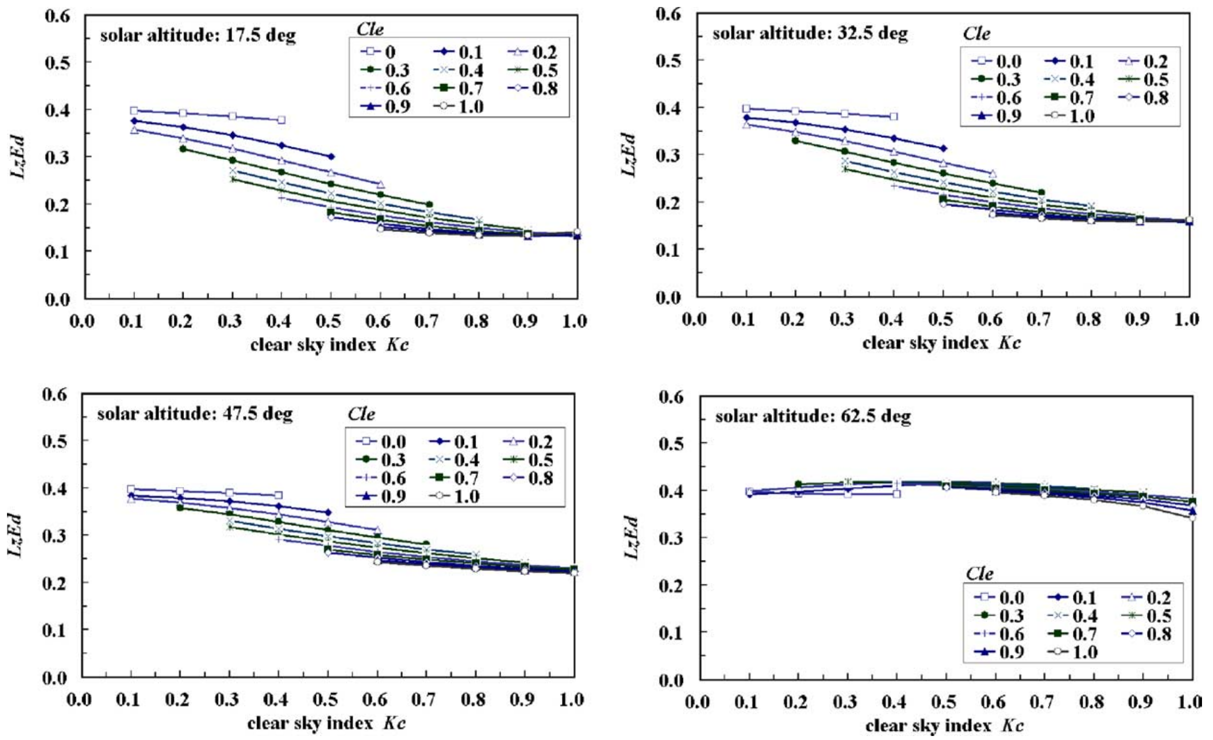


Fig. 8. LzEds for clear sky index and cloudless index.

Tokyo. Fig. 7 shows an example of the relationship between the clear sky index and the root of cloudless index in Kagoshima (1995/1–2001/12). The primary relationship is found between them. The sum of the clear sky index and root of cloudless index is defined as the sky index (Si). Coefficients *a*, *b*, *c*, *d* and *e* are obtained as a function of the sky index.

The sky radiance distribution shown in absolute value for all sky conditions referred to hereafter as the All Sky Model-R is composed by multiplying the relative sky radiance distribution and the zenith radiance as follows:

$$\mathrm{Lea}(\gamma_s,\gamma,\zeta) = \mathrm{Lez}(\gamma_s)\cdot \mathrm{Le}(\gamma_s,\gamma,\zeta) = \mathrm{Lez}(\gamma_s)\cdot \frac{\phi(\gamma)\cdot f(\zeta)}{\phi(\pi/2)\cdot f(\pi/2-\gamma_s)} \qquad (9)$$

where

$\mathrm{Lea}(\gamma_s,\gamma,\zeta)$ is the sky radiance distribution of the All Sky Model-R ($W/m^2$ sr),
$\mathrm{Lez}(\gamma_s)$ the zenith radiance ($W/m^2$ sr),
$\mathrm{Le}(\gamma_s,\gamma,\zeta)$ the relative sky radiance distribution,
$\phi(\gamma) = 1 + a\cdot\exp(b/\sin\gamma)$ the gradation function,
$f(\zeta) = 1 + c\cdot[\exp(d\cdot\zeta) - \exp(d\cdot\pi/2)] + e\cdot\cos^2\zeta$ the scattering indicatrix function,
$a = 4.5/[1 + 0.15\cdot\exp(3.4\cdot\mathrm{Si})] - 1.04$,
$b = -1/[1 + 0.17\cdot\exp(1.3\cdot\mathrm{Si})] - 0.05$,
$c = 1.77\cdot(1.22\cdot\mathrm{Si})^{3.56}\cdot\exp(0.2\cdot\mathrm{Si})\cdot(2.1-\mathrm{Si})^{0.8}$,
$d = -3.05/[1 + 10.6\cdot\exp(-3.4\cdot\mathrm{Si})]$,
$e = 0.48/[1 + 245\cdot\exp(-4.13\cdot\mathrm{Si})]$,
$\mathrm{Si} = \mathrm{Kc} + \mathrm{Cle}^{0.5}$ the sky index,
$\mathrm{Kc} = \mathrm{Eeg}/\mathrm{Seeg}$ the clear sky index,
Eeg the global irradiance ($W/m^2$),
$\mathrm{Seeg} = 0.84\cdot\mathrm{Eeo}/m\cdot\exp(-0.0675\cdot m)$ the standard global irradiance ($W/m^2$),
$m = 1/[\cos\gamma_{sz} + 0.50572\cdot(96.07995-\gamma_{sz})^{-1.6364}]$ the relative optical air mass,
$\gamma_{sz}$ the zenith angle of the sun (deg),
$\mathrm{Cle} = (1-\mathrm{Ce})/(1-\mathrm{Ce_s})$ the cloudless index,
$\mathrm{Ce} = \mathrm{Eed}/\mathrm{Eeg}$ the cloud ratio,
Eed the diffuse irradiance ($W/m^2$),
$\mathrm{Ce_s} = 0.01299 + 0.07698\cdot m - 0.003857\cdot m^2 + 0.0001054\cdot m^3 - 0.000001031\cdot m^4$ the standard cloud ratio,
$\gamma_s$ the solar altitude (rad),
$\gamma$ the altitude of the sky element (rad),
$\zeta = \arccos(\sin\gamma_s\cdot\sin\gamma + \cos\gamma_s\cdot\cos\gamma\cdot\cos|\alpha_s-\alpha|)$ the angular distance between the sun and the sky element (rad),
$\alpha_s$ the azimuth angle of the sun (rad),
$\alpha$ the azimuth angle of the sky element (rad).

Table 1
Coefficients for LzEd

| k | j | i: 5 | 4 | 3 | 2 | 1 | 0 |
|---|---|---|---|---|---|---|---|
| 4 | 6 | −79.2551 | 181.5249 | −178.8391 | 86.4222 | 13.7469 | −9.3016 |
| | 5 | 259.0233 | −599.2154 | 558.7982 | −273.5933 | −28.3222 | 36.8154 |
| | 4 | −323.9300 | 758.4764 | −665.1001 | 327.9505 | 2.5328 | −52.2028 |
| | 3 | 178.5947 | −422.7656 | 343.9805 | −171.1919 | 27.4527 | 32.8606 |
| | 2 | −34.0204 | 80.2519 | −57.2731 | 28.9888 | −17.6413 | −8.0731 |
| | 1 | −0.9299 | 2.9337 | −2.7390 | 2.0469 | 1.9924 | −0.1519 |
| | 0 | −0.0673 | 0.1200 | −0.5003 | −0.0077 | 0.2274 | 0.1944 |
| 3 | 6 | 178.9761 | −414.3978 | 382.3517 | −189.0674 | −19.1604 | 26.7019 |
| | 5 | −585.76778 | 1369.3651 | −1197.9089 | 597.8211 | 18.6492 | −98.6168 |
| | 4 | 719.1565 | −1698.4940 | 1398.0054 | −701.8434 | 57.7891 | 133.1647 |
| | 3 | −377.9488 | 899.2027 | −681.3328 | 345.6662 | −99.9641 | −79.6806 |
| | 2 | 63.7066 | −149.2886 | 93.5278 | −47.5262 | 47.1414 | 17.6094 |
| | 1 | 2.2956 | −7.2571 | 6.1345 | −5.5006 | −4.1306 | 1.0003 |
| | 0 | 0.4479 | −1.0320 | 1.7185 | −0.3234 | −0.5077 | −0.3754 |
| 2 | 6 | −140.1650 | 329.5323 | −283.3008 | 142.5802 | 0.0588 | −24.2309 |
| | 5 | 450.5763 | −1067.6426 | 872.1058 | −442.3932 | 38.0638 | 85.2745 |
| | 4 | −530.7575 | 1266.6167 | −971.1740 | 496.1507 | −112.2037 | −109.9849 |
| | 3 | 258.3140 | −617.6864 | 428.3022 | −220.7694 | 112.7302 | 61.4569 |
| | 2 | −37.2452 | 86.0313 | −44.2429 | 20.6861 | −41.5866 | −11.1184 |
| | 1 | −1.1026 | 3.9671 | −2.6865 | 3.9616 | 2.8287 | −1.2699 |
| | 0 | −0.3572 | 0.8603 | −1.0970 | 0.3359 | 0.3435 | 0.0863 |
| 1 | 6 | 41.7667 | −101.3222 | 83.3628 | −44.0612 | 8.0616 | 7.8350 |
| | 5 | −128.3895 | 313.3116 | −245.8816 | 131.5008 | −38.0729 | −26.2167 |
| | 4 | 140.6794 | −344.9908 | 254.2300 | −137.6762 | 64.8618 | 31.5218 |
| | 3 | −61.5252 | 150.9138 | −100.4209 | 54.5553 | −48.3263 | −15.2722 |
| | 2 | 7.8043 | −18.4959 | 9.7897 | −3.9888 | 14.3852 | 1.6549 |
| | 1 | 0.1990 | −0.7237 | 0.3678 | −0.8060 | −0.8417 | 0.2509 |
| | 0 | 0.0888 | −0.2173 | 0.2446 | −0.0842 | −0.0767 | −0.0509 |
| 0 | 6 | −2.3236 | 3.8397 | 1.3678 | −2.8773 | 0.5302 | −0.9167 |
| | 5 | 5.9466 | −8.4370 | −8.4637 | 11.3017 | −0.8960 | 2.7842 |
| | 4 | −4.8599 | 4.1516 | 15.9467 | −16.8828 | 0.0930 | −2.8711 |
| | 3 | 1.1362 | 1.8522 | −12.3903 | 11.6859 | 0.3772 | 1.0626 |
| | 2 | 0.2833 | −1.9825 | 4.3546 | −3.7111 | −0.0829 | −0.1460 |
| | 1 | −0.0817 | 0.3300 | −0.4699 | 0.4062 | −0.0316 | −0.0564 |
| | 0 | −0.0068 | 0.0177 | −0.0200 | 0.0090 | 0.0044 | 0.4015 |

The zenith radiance can be shown by dividing the diffuse irradiance by the integration value of the relative sky radiance distribution.

$$\mathrm{Lez}(\gamma_s) = \frac{\mathrm{Eed}}{\int_{\gamma=0}^{\pi/2}\int_{\alpha=0}^{2\pi} \mathrm{Le}(\gamma_s,\gamma,\zeta)\cdot\sin\gamma\cdot\cos\gamma\cdot \mathrm{d}\gamma\cdot\mathrm{d}\alpha} \quad (10)$$

If the integration value of the relative sky radiance distribution is prepared, the zenith radiance is easily calculated. The zenith radiance is shown as functions of the solar altitude, the clear sky index and the cloudless index as follows:

$$\mathrm{Lez}(\gamma_s, \mathrm{Kc}, \mathrm{Cle}) = \mathrm{Eed}\cdot\mathrm{LzEd} \quad (11)$$

where $\mathrm{Lez}(\gamma_s, \mathrm{Kc}, \mathrm{Cle})$ is the zenith radiance of the All Sky Model-R (W/m$^2$ sr),

$$\mathrm{LzEd} = \frac{1}{\int_{\gamma=0}^{\pi/2}\int_{\alpha=0}^{2\pi} \mathrm{Le}(\gamma_s,\gamma,\zeta)\cdot\sin\gamma\cdot\cos\gamma\cdot \mathrm{d}\gamma\cdot\mathrm{d}\alpha}.$$

LzEds are calculated in all the classified sky conditions. The examples of *LzEd* when the solar altitudes are 17.5°, 32.5°, 47.5° and 62.5° are shown in Fig. 8. LzEd seems to be shown as functions of Kc, Cle and the solar altitude.

LzEd obtained by the calculation is analyzed by the next equation as a function of Kc.

$$\mathrm{LzEd} = \sum_{k=0}^{4}[A(k)\cdot \mathrm{Kc}^k] \quad (12)$$

$A(0) \sim A(4)$ coefficients.

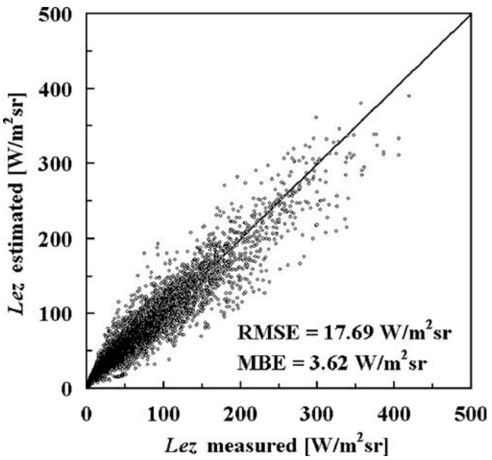


Fig. 9. The zenith radiance measured and calculated.

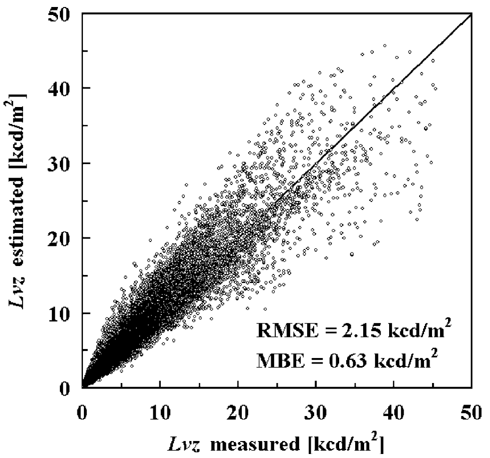


Fig. 10. The zenith luminance measured and calculated.

Subsequently, $A(k)$ is analyzed by the next equation as a function of Cle.

$$A(k) = \sum_{j=0}^{6}[B(j,k) \cdot \mathrm{Cle}^{0.5 \cdot j}] \tag{13}$$

$B(0,k) \sim B(6,k)$ coefficients.

In addition, $B(j,k)$ is analyzed by the next equation as a function of the solar altitude

$$B(j,k) = \sum_{i=0}^{5}[C(i,j,k) \cdot \gamma_s^i] \tag{14}$$

$C(0,j,k) \sim C(5,j,k)$ coefficients. Here, substituting $C(i,j,k)$ for Eq. (14), $B(j,k)$ is obtained. And, substituting $B(j,k)$ for Eq. (13), $A(k)$ is obtained and $A(4)$ is fixed. Moreover, repeating a similar method, all the coefficients are fixed. Finally, LzEd is shown as follows:

$$\mathrm{LzEd} = \sum_{k=0}^{4}[A(k) \cdot \mathrm{Kc}^k] \tag{15}$$

With $A(k) = \sum_{j=0}^{6}[B(j,k) \cdot \mathrm{Cle}^{0.5 \cdot j}]$, $B(j,k) = \sum_{i=0}^{5}[C(i,j,k) \cdot \gamma_s^i]$.

The coefficient $C(i,j,k)$ for LzEd is shown in Table 1. LzEd will be calculated in a short time because the integration of Eq. (10) is not necessary. The zenith radiance is shown as follows:

$$\mathrm{Lez}(\gamma_s, \mathrm{Kc}, \mathrm{Cle}) = \mathrm{Eed} \cdot \mathrm{LzEd} = \mathrm{Eed} \cdot \sum_{k=0}^{4}[A(k) \cdot \mathrm{Kc}^k]. \tag{16}$$

The relation between the measurement value of the zenith radiance in Tokyo and the calculation value by Eq. (16) is shown in Fig. 9. A good result is obtained as the estimation value of the zenith radiance with 17.69 W/m$^2$ sr of RMSE and 3.62 W/m$^2$ sr of MSE.

### 4.2. Formulation of sky luminance distribution

Following the relative sky luminance distribution, the sky luminance distribution shown in absolute value for all sky conditions referred to hereafter as the All Sky Model-L can be composed as follows:

$$\begin{aligned}\mathrm{Lva}(\gamma_s, \gamma, \zeta) &= \mathrm{Lvz}(\gamma_s) \cdot \mathrm{Lv}(\gamma_s, \gamma, \zeta) \\ &= \mathrm{Lvz}(\gamma_s) \cdot \frac{\phi(\gamma) \cdot f(\zeta)}{\phi(\pi/2) \cdot f(\pi/2 - \gamma_s)}\end{aligned} \tag{17}$$

where $\mathrm{Lva}(\gamma_s, \gamma, \zeta)$ is the sky luminance distribution of the All Sky Model-L (cd/m$^2$), $\mathrm{Lvz}(\gamma_s)$ the zenith luminance (cd/m$^2$) and $\mathrm{Lv}(\gamma_s, \gamma, \zeta)$ the relative sky luminance distribution ($= \mathrm{Le}(\gamma_s, \gamma, \zeta)$).

The zenith luminance can be shown by composition similar to the zenith radiance as follows:

$$\mathrm{Lvz}(\gamma_s) = \frac{\mathrm{Evd}}{\int_{\gamma=0}^{\pi/2}\int_{\alpha=0}^{2\pi} \mathrm{Lv}(\gamma_s, \gamma, \zeta) \cdot \sin\gamma \cdot \cos\gamma \cdot d\gamma \cdot d\alpha} \tag{18}$$

where Evd is the diffuse illuminance (lx).

Since the diffuse illuminance is calculated by multiplying the diffuse luminous efficacy and diffuse irradiance, the zenith luminance can be obtained by the same composition to Eq. (16) as follows:

$$\begin{aligned}\mathrm{Lvz}(\gamma_s, \mathrm{Kc}, \mathrm{Cle}) &= \mathrm{Evd} \cdot \mathrm{LzEd} \\ &= \eta_d \cdot \mathrm{Eed} \cdot \sum_{k=0}^{4}[A(k) \cdot \mathrm{Kc}^k]\end{aligned} \tag{19}$$

where $\eta_d$ is the diffuse luminous efficacy (lm/W).

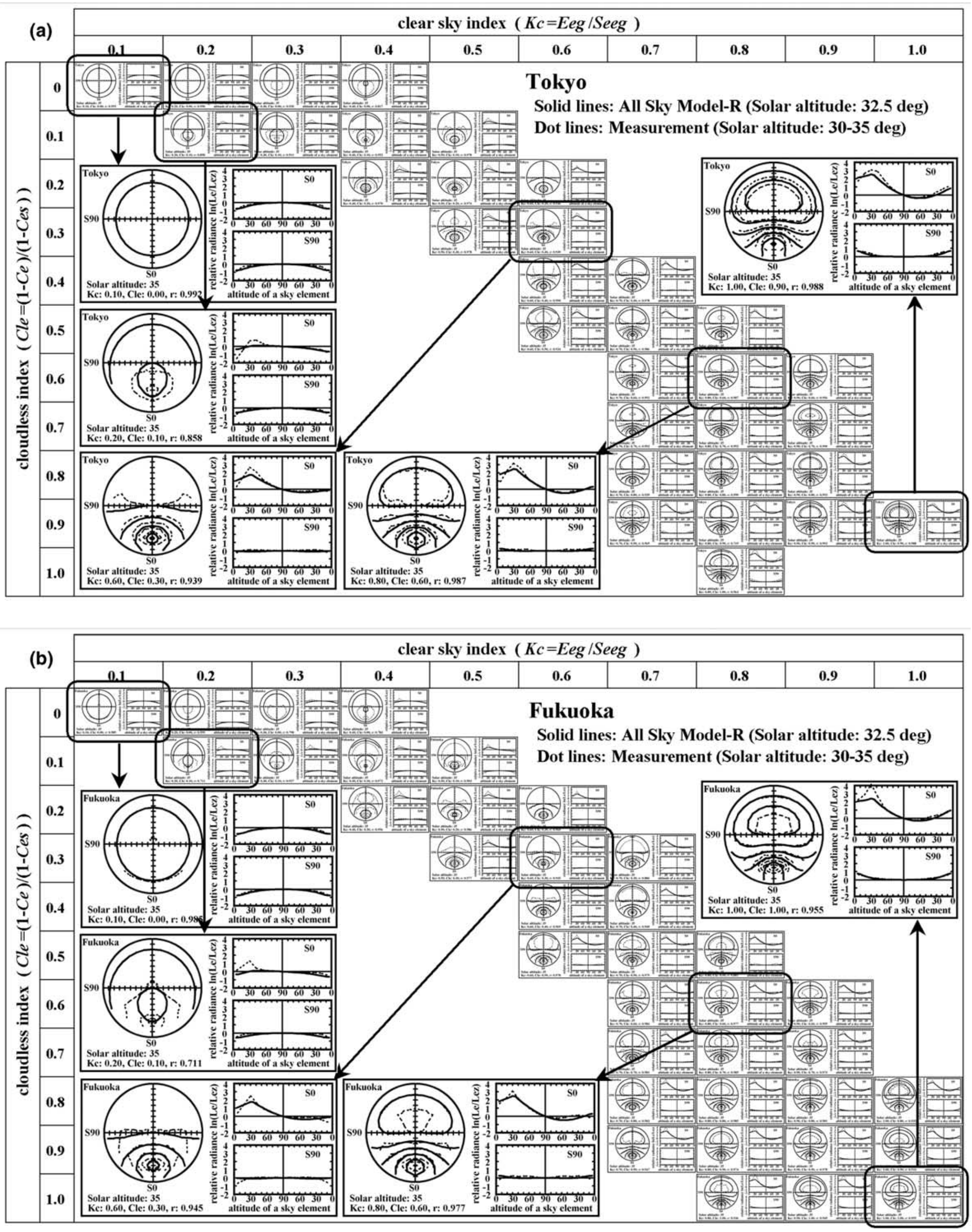


Fig. 11. Comparison of the relative sky radiance distribution between the All Sky Model-R and measurements in Tokyo and Fukuoka.

The relation between the measurement values of the zenith luminance in Tokyo and the calculation values by Eq. (19) is shown in Fig. 10 with 2.15 kcd/m$^2$ of RMSE and 0.63 kcd/m$^2$ of MBE.

## 5. Validation of "All Sky Model"

The examples of the relationship of the relative sky radiance distribution at 32.5° of the solar altitude between the calculation values of the All Sky Model-R and the measurement values in Tokyo and Fukuoka are shown in Fig. 11 where the validation in Tokyo is not entirely independent. The measurements and the calculations are corresponding very well. A similar tendency is shown in other solar altitudes. Moreover, a similar result is obtained in the comparison between the All Sky Model-L and the measurement value concerning the relative sky luminance distribution.

As shown in Fig. 12, the sky conditions are tentatively classified into five categories: (1) clear sky conditions ($Si \geqslant 1.7$), (2) near clear sky conditions ($1.7 \geqslant Si > 1.5$), (3) intermediate sky conditions ($1.5 \geqslant Si > 0.6$), (4) near overcast sky conditions ($0.6 \geqslant Si > 0.3$), and (5) overcast sky conditions ($Si \leqslant 0.3$). And the sky vault is divided into four regions: (a) the zenith region: the sky element of which altitude is higher than 60° above the horizon, (b) the south region: the region in the direction of the sun (azimuth < 45° and altitude < 60°), (c) the north region: the region opposite to the sun region (azimuth > 135° and altitude < 60°), (d) the east–west region: the region on the both sides of the sun (45° < azimuth < 135° and altitude < 60°).

Based on the basic data for the formulation of sky radiance and luminance distributions at solar altitude from 20° to 70 °, MBE and RMSE are calculated between the estimation values of All Sky Model-R, All Sky Model-L, Perez Model (1993); Brunger Model (1993); Harrison Model (1991); Kittler Model (1986); and Perraudeau Model (1988) where the validation of the All Sky Model-R in Tokyo is not entirely independent. For the Harrison model the difference between one and cloudless index was assumed to be the opaque cloud cover. The data of the sky elements at 6° altitude are excluded. The data of which the angular distance between the sun and the sky element is smaller than 15 degrees are excluded. Because the angular distance between the sun and the zenith is small when the solar altitude is higher than 70°, the accuracy of measurements of the zenith radiance (luminance) cannot be secured and the data are excluded.

The results of the model validation of sky radiance and luminance distributions are shown in Tables 2 and 3. The summary of model validation of radiance distributions is shown in Table 4 and Fig. 13. The summary of model validation of luminance distributions is shown in Table 5 and Fig. 14. In all the model validation, All Sky Model-R and All Sky Model-L are found to have good accuracy for the sky radiance and luminance distributions. Perez Model and Brunger Model are also found of their good accuracy. In all the sky conditions except the near clear sky, All Sky Model-R and All Sky Model-L obtained the best

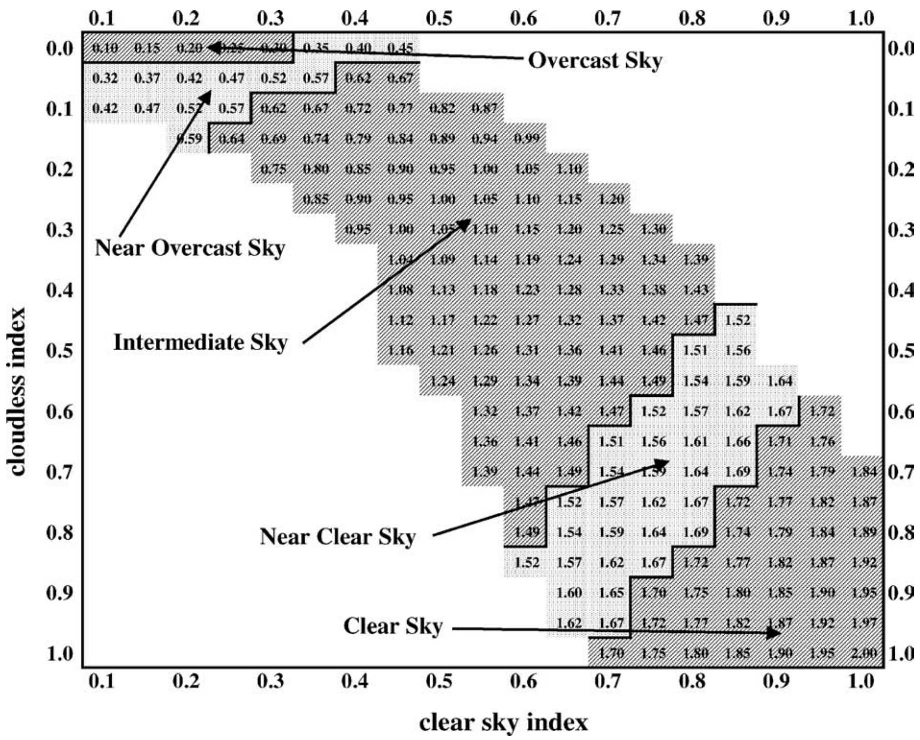


Fig. 12. Classification of sky conditions for Si. (The values in the figure indicate the sky index Si.)

Table 2
Model validation of sky radiance distributions

| | Entire | | Zenith | | South | | North | | East-West | |
|---|---|---|---|---|---|---|---|---|---|---|
| | MBE | RMSE | MBE | RMSE | MBE | RMSE | MBE | RMSE | MBE | RMSE |
| *Clear sky conditions* | | | | | | | | | | |
| All Sky Model-R | 0.19 | 8.46 | 0.47 | 7.53 | 1.73 | 15.35 | −1.51 | 4.97 | 0.34 | 5.11 |
| Perez | 0.35 | 8.46 | 0.21 | 7.39 | −4.53 | 15.18 | 2.28 | 5.36 | 1.63 | 5.20 |
| Brunger | −0.38 | 9.50 | 0.95 | 9.06 | −4.82 | 17.11 | 1.18 | 5.41 | 0.29 | 5.61 |
| Harrison | 0.14 | 10.99 | 0.89 | 8.49 | −11.15 | 20.14 | 4.96 | 8.32 | 2.45 | 5.78 |
| Kittler | −0.26 | 9.42 | 2.20 | 8.65 | −6.65 | 17.65 | 1.02 | 4.92 | 1.07 | 4.98 |
| Perraudeau | 0.50 | 11.75 | −1.31 | 10.39 | −5.74 | 21.73 | 2.93 | 6.78 | 2.83 | 6.59 |
| Mean radiance | 33.14 | | 28.58 | | 69.56 | | 18.81 | | 25.86 | |
| Number of data | 18,846 | | 3140 | | 3666 | | 4472 | | 7568 | |
| Number of sets | 172 | | | | | | | | | |
| *Near clear sky conditions* | | | | | | | | | | |
| All Sky Model-R | 0.64 | 11.70 | 0.18 | 10.51 | 5.00 | 21.22 | −1.57 | 6.58 | 0.01 | 7.13 |
| Perez | 0.83 | 10.93 | −0.92 | 10.63 | −4.79 | 18.40 | 4.15 | 7.37 | 2.32 | 7.37 |
| Brunger | −0.17 | 12.70 | 1.15 | 12.26 | −7.80 | 22.26 | 4.12 | 7.84 | 0.46 | 7.90 |
| Harrison | 0.53 | 17.27 | 0.99 | 13.94 | −20.95 | 31.18 | 10.91 | 13.45 | 4.63 | 9.12 |
| Kittler | −0.04 | 16.96 | 1.05 | 14.95 | −19.83 | 30.84 | 8.82 | 11.84 | 3.90 | 8.90 |
| Perraudeau | 1.66 | 18.73 | −5.28 | 17.41 | −14.78 | 31.66 | 10.83 | 14.20 | 7.10 | 11.92 |
| Mean radiance | 53.15 | | 50.57 | | 108.45 | | 28.74 | | 41.78 | |
| Number of data | 17,543 | | 2922 | | 3421 | | 4160 | | 7040 | |
| Number of sets | 160 | | | | | | | | | |
| *Intermediate sky conditions* | | | | | | | | | | |
| All Sky Model-R | 0.76 | 13.75 | 1.11 | 12.35 | 0.59 | 23.57 | −0.13 | 8.90 | 1.23 | 9.53 |
| Perez | 2.02 | 16.77 | −3.41 | 14.56 | 11.58 | 29.48 | −0.50 | 10.67 | 1.11 | 11.10 |
| Brunger | 0.22 | 17.51 | 2.01 | 19.54 | 3.43 | 29.01 | −1.09 | 11.36 | −1.32 | 10.97 |
| Harrison | 0.88 | 17.61 | 0.98 | 14.67 | −17.20 | 30.68 | 10.04 | 13.43 | 4.23 | 10.91 |
| Kittler | 0.72 | 26.20 | −2.21 | 23.30 | −33.08 | 44.73 | 18.57 | 21.82 | 7.83 | 15.20 |
| Perraudeau | 4.50 | 22.62 | −12.29 | 20.96 | −2.00 | 32.89 | 12.47 | 19.88 | 9.92 | 18.26 |
| Mean radiance | 71.48 | | 77.60 | | 119.59 | | 46.92 | | 60.04 | |
| Number of data | 33,219 | | 5524 | | 6485 | | 7878 | | 13,332 | |
| Number of sets | 303 | | | | | | | | | |
| *Near overcast sky conditions* | | | | | | | | | | |
| All Sky Model-R | 0.16 | 8.69 | −0.29 | 8.51 | −4.23 | 12.75 | 2.90 | 7.15 | 0.86 | 6.99 |
| Perez | 1.28 | 8.83 | −3.50 | 8.82 | 3.15 | 12.56 | 0.99 | 6.71 | 2.53 | 7.66 |
| Brunger | 0.22 | 9.34 | 0.49 | 8.60 | 1.06 | 13.51 | −0.63 | 7.43 | 0.20 | 8.08 |
| Harrison | 1.18 | 10.84 | −2.12 | 9.95 | 9.68 | 17.46 | −1.38 | 8.26 | −0.08 | 7.94 |
| Kittler | −0.07 | 10.53 | 0.01 | 10.19 | −8.93 | 15.95 | 5.53 | 9.29 | 0.89 | 7.66 |
| Perraudeau | 4.36 | 16.62 | −11.83 | 16.10 | 6.03 | 18.82 | 8.69 | 16.31 | 7.69 | 15.85 |
| Mean radiance | 57.81 | | 71.02 | | 64.69 | | 50.20 | | 53.48 | |
| Number of data | 14,143 | | 2354 | | 2759 | | 3354 | | 5676 | |
| Number of sets | 129 | | | | | | | | | |
| *Overcast sky conditions* | | | | | | | | | | |
| All Sky Model-R | −0.34 | 3.71 | 0.79 | 3.13 | −0.24 | 3.88 | −0.65 | 3.95 | −0.68 | 3.70 |
| Perez | 0.45 | 3.82 | −1.50 | 3.42 | 1.74 | 4.62 | 0.06 | 3.62 | 0.86 | 3.66 |
| Brunger | 0.20 | 3.53 | −0.31 | 3.06 | 0.46 | 3.94 | 0.19 | 3.53 | 0.30 | 3.49 |
| Harrison | 0.33 | 6.85 | −0.44 | 6.06 | 8.38 | 11.04 | −3.65 | 6.00 | −0.92 | 4.57 |
| Kittler | −0.41 | 3.81 | 1.35 | 3.47 | −0.61 | 3.89 | −0.74 | 4.02 | −0.85 | 3.77 |
| Perraudeau | 1.86 | 7.01 | −5.07 | 6.50 | 6.07 | 9.07 | 1.46 | 5.91 | 2.90 | 6.64 |
| Mean radiance | 27.70 | | 33.42 | | 26.62 | | 26.91 | | 26.32 | |
| Number of data | 7125 | | 1181 | | 1394 | | 1690 | | 2860 | |
| Number of sets | 65 | | | | | | | | | |

Table 3
Model validation of sky luminance distributions

| | Entire | | Zenith | | South | | North | | East-West | |
|---|---|---|---|---|---|---|---|---|---|---|
| | MBE | RMSE | MBE | RMSE | MBE | RMSE | MBE | RMSE | MBE | RMSE |
| *Clear sky conditions* | | | | | | | | | | |
| All Sky Model-L | −22 | 809 | 134 | 858 | 64 | 1464 | −177 | 401 | −36 | 435 |
| Perez | 1 | 873 | 91 | 840 | −699 | 1606 | 299 | 494 | 128 | 457 |
| Brunger | −94 | 1081 | 198 | 1071 | −751 | 2005 | 160 | 487 | −46 | 587 |
| Harrison | −26 | 1280 | 177 | 1029 | −1510 | 2410 | 620 | 903 | 226 | 585 |
| Kittler | −77 | 1038 | 345 | 1035 | −972 | 1979 | 139 | 459 | 55 | 462 |
| Perraudeau | 8 | 1346 | −99 | 1244 | −864 | 2521 | 364 | 743 | 264 | 681 |
| Mean luminance | 4167 | | 3498 | | 8779 | | 2326 | | 3295 | |
| Number of data | 19,285 | | 3212 | | 3753 | | 4576 | | 7744 | |
| Number of sets | 176 | | | | | | | | | |
| *Near clear sky conditions* | | | | | | | | | | |
| All Sky Model-L | 38 | 1230 | 78 | 1219 | 521 | 2223 | −184 | 669 | −82 | 695 |
| Perez | 70 | 1172 | −79 | 1233 | −698 | 1938 | 553 | 833 | 220 | 746 |
| Brunger | −64 | 1527 | 208 | 1526 | −1078 | 2700 | 535 | 895 | −38 | 912 |
| Harrison | 29 | 2081 | 164 | 1703 | −2732 | 3780 | 1397 | 1626 | 510 | 1033 |
| Kittler | −45 | 2058 | 181 | 1836 | −2623 | 3737 | 1143 | 1466 | 415 | 1044 |
| Perraudeau | 192 | 2257 | −613 | 2158 | −1922 | 3786 | 1401 | 1754 | 840 | 1405 |
| Mean luminance | 6844 | | 6456 | | 13,939 | | 3661 | | 5433 | |
| Number of data | 17,762 | | 2953 | | 3469 | | 4212 | | 7128 | |
| Number of sets | 162 | | | | | | | | | |
| *Intermediate sky conditions* | | | | | | | | | | |
| All Sky Model-L | 44 | 1263 | 203 | 1223 | 99 | 2147 | −50 | 831 | 8 | 838 |
| Perez | 207 | 1701 | −360 | 1515 | 1361 | 3021 | −40 | 1096 | 25 | 1053 |
| Brunger | −20 | 1924 | 309 | 2219 | 458 | 3197 | −168 | 1219 | −302 | 1153 |
| Harrison | 60 | 1876 | 185 | 1577 | −2044 | 3297 | 1178 | 1494 | 372 | 1063 |
| Kittler | 41 | 2975 | −205 | 2644 | −3965 | 5085 | 2216 | 2552 | 808 | 1652 |
| Perraudeau | 498 | 2436 | −1422 | 2336 | −212 | 3457 | 1471 | 2251 | 1063 | 1928 |
| Mean luminance | 8724 | | 9358 | | 14,476 | | 5731 | | 7429 | |
| Number of data | 33,438 | | 5555 | | 6533 | | 7930 | | 13,420 | |
| Number of sets | 305 | | | | | | | | | |
| *Near overcast sky conditions* | | | | | | | | | | |
| All Sky Model-L | −27 | 902 | 34 | 864 | −486 | 1357 | 263 | 740 | 0 | 705 |
| Perez | 95 | 907 | −311 | 896 | 322 | 1351 | 43 | 666 | 184 | 753 |
| Brunger | −18 | 984 | 124 | 897 | 147 | 1399 | −156 | 820 | −76 | 856 |
| Harrison | 97 | 1201 | −186 | 1118 | 1219 | 2006 | −265 | 895 | −118 | 803 |
| Kittler | −55 | 1145 | 67 | 1071 | −1059 | 1777 | 585 | 1007 | 4 | 808 |
| Perraudeau | 488 | 1860 | −1382 | 1824 | 789 | 2147 | 965 | 1830 | 836 | 1737 |
| Mean luminance | 7136 | | 8634 | | 7902 | | 6250 | | 6665 | |
| Number of data | 14,143 | | 2354 | | 2759 | | 3354 | | 5676 | |
| Number of sets | 129 | | | | | | | | | |
| *Overcast sky conditions* | | | | | | | | | | |
| All Sky Model-L | −58 | 444 | 109 | 360 | −47 | 468 | −92 | 470 | −112 | 446 |
| Perez | 46 | 429 | −191 | 389 | 207 | 538 | 3 | 401 | 90 | 400 |
| Brunger | 13 | 391 | −33 | 339 | 43 | 452 | 17 | 386 | 15 | 380 |
| Harrison | 30 | 857 | −50 | 778 | 1078 | 1402 | −486 | 745 | −144 | 543 |
| Kittler | −67 | 459 | 179 | 415 | −95 | 472 | −103 | 481 | −133 | 457 |
| Perraudeau | 229 | 845 | −656 | 807 | 111 | 1123 | 183 | 693 | 356 | 783 |
| Mean luminance | 3637 | | 4361 | | 3503 | | 3530 | | 3468 | |
| Number of data | 7236 | | 1200 | | 1416 | | 1716 | | 2904 | |
| Number of sets | 66 | | | | | | | | | |

Table 4
Summary of model validations of radiance distributions: mean bias errors, root mean square errors, and mean sky radiance [W/m²sr]

| | Whole sky | | Clear sky | | Near clear sky | | Intermediate sky | | Near overcast sky | | Overcast sky | |
|---|---|---|---|---|---|---|---|---|---|---|---|---|
| | MBE | RMSE | MBE | RMSE | MBE | RMSE | MBE | RMSE | MBE | RMSE | MBE | RMSE |
| All Sky Model-R | 0.44 | 11.10 | 0.19 | 8.46 | 0.64 | 11.70 | 0.76 | 13.75 | 0.16 | 8.69 | −0.34 | 3.71 |
| Perez | 1.21 | 12.41 | 0.35 | 8.46 | 0.83 | 10.93 | 2.02 | 16.77 | 1.28 | 8.83 | 0.45 | 3.82 |
| Brunger | 0.02 | 13.29 | −0.38 | 9.50 | −0.17 | 12.70 | 0.22 | 17.51 | 0.22 | 9.34 | 0.20 | 3.53 |
| Harrison | 0.66 | 14.76 | 0.14 | 10.99 | 0.53 | 17.27 | 0.88 | 17.61 | 1.18 | 10.84 | 0.33 | 6.85 |
| Kittler | 0.16 | 18.53 | −0.26 | 9.42 | −0.04 | 16.96 | 0.72 | 26.20 | −0.07 | 10.53 | −0.41 | 3.81 |
| Perraudeau | 2.89 | 18.17 | 0.50 | 11.75 | 1.66 | 18.73 | 4.50 | 22.62 | 4.36 | 16.62 | 1.86 | 7.01 |
| Mean radiance | 54.43 | | 33.14 | | 53.15 | | 71.48 | | 57.81 | | 27.70 | |
| Number of data | 90,876 | | 18,846 | | 17,543 | | 33,219 | | 14,143 | | 7125 | |
| Number of sets | 829 | | 172 | | 160 | | 303 | | 129 | | 65 | |

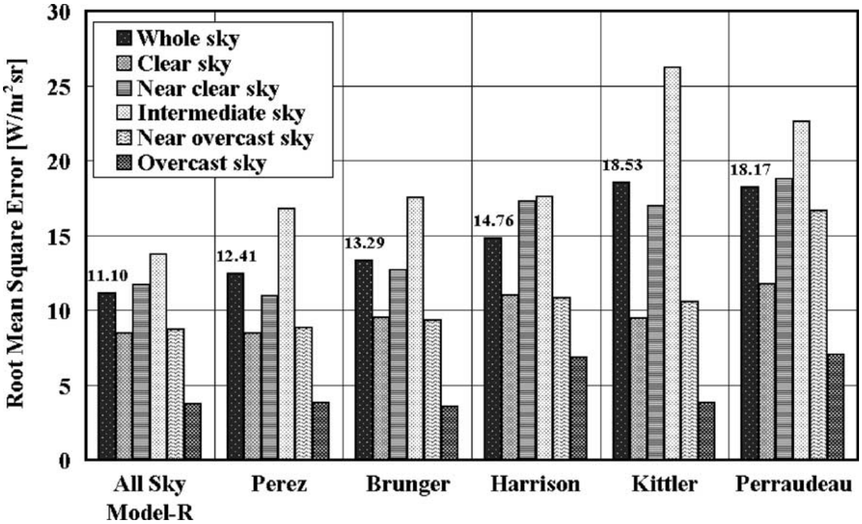


Fig. 13. Comparison of models for sky radiance distributions.

results. Though Perez Model obtained the best results in the near clear sky, the differences with All Sky Models are very small.

For each classified area, coefficients of correlation between the All Sky Model-L and 15 Types of the CIE Standard General Sky are calculated. The Type of the General Sky that shows the largest coefficient of correlation is selected to compare with the All Sky Model-L. The relative sky luminance distribution of the All Sky Model-L and the most similar sky type of the CIE Standard General Sky is shown in Fig. 15. The All Sky Model-L is corresponding to Type 1 in the overcast sky, and to Type 12 in the clear sky, which they are the previous Standard Skies. In the All Sky Model-L, neither Type 5 nor Type 15 appears. Type 5 is the uniform sky, and does not appear originally. Moreover, Type 15 is the special distribution, and scarcely appears actually. Substantially, the All Sky Model-L contains the most Types of the CIE Standard General Sky.

In addition, the measurement values and estimation values by the All Sky Model-R, the Perez Model (1990), and the Isotropic Model are compared for the vertical irradiances on the north, the east, the south, and the west surfaces. The sum of the calculated vertical diffuse irradiance of each model and the vertical direct irradiance calculated by the direct normal irradiance measured is assumed to be the estimation value of the vertical irradiance. The examples of the comparison for the clear sky days (November 23, 1992 June 10, 1993 and September 27) and the turbid sky day (November

Table 5
Summary of model validations of luminance distributions: mean bias errors, root mean square errors, andmean sky luminance [cd/m$^2$]

| | Whole sky | | Clear sky | | Near clear sky | | Intermediate sky | | Near overcast sky | | Overcast sky | |
|---|---|---|---|---|---|---|---|---|---|---|---|---|
| | MBE | RMSE | MBE | RMSE | MBE | RMSE | MBE | RMSE | MBE | RMSE | MBE | RMSE |
| All Sky Model-L | 10 | 1073 | −22 | 809 | 38 | 1230 | 44 | 1263 | −27 | 902 | −58 | 444 |
| Perez | 107 | 1273 | 1 | 873 | 70 | 1172 | 207 | 1701 | 95 | 907 | 46 | 429 |
| Brunger | −41 | 1485 | −94 | 1081 | −64 | 1527 | −20 | 1924 | −18 | 984 | 13 | 391 |
| Harrison | 39 | 1656 | −26 | 1280 | 29 | 2081 | 60 | 1876 | 97 | 1201 | 30 | 857 |
| Kittler | −24 | 2118 | −77 | 1038 | −45 | 2058 | 41 | 2975 | −55 | 1145 | −67 | 459 |
| Perraudeau | 313 | 2028 | 8 | 1346 | 192 | 2257 | 498 | 2436 | 488 | 1860 | 229 | 845 |
| Mean luminance | 6758 | | 4167 | | 6844 | | 8724 | | 7136 | | 3637 | |
| Number of data | 91,864 | | 19,285 | | 17,762 | | 33,438 | | 14,143 | | 7236 | |
| Number of sets | 838 | | 176 | | 162 | | 305 | | 129 | | 66 | |

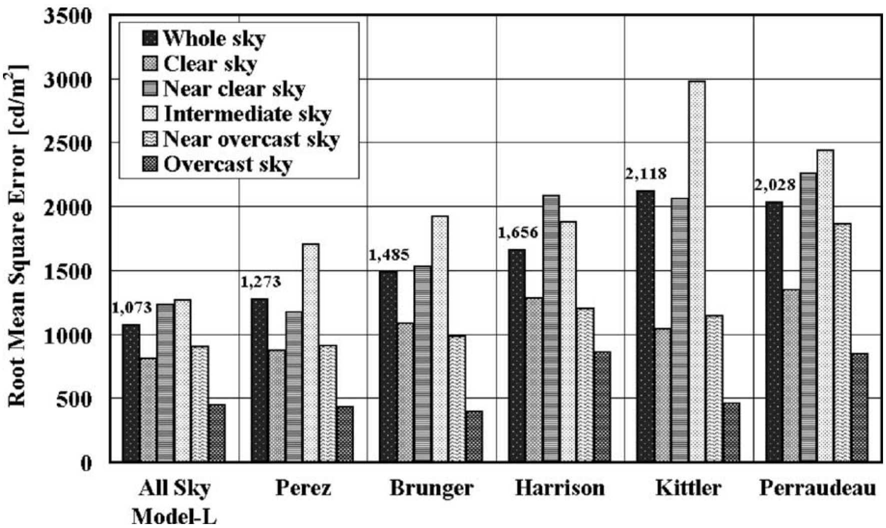


Fig. 14. Comparison of models for sky luminance distributions.

23, 1992) based on the measurement data in Tokyo are shown in Fig. 16.

The estimation value of the Isotropic Model is different from an actual phenomenon. For instance, the Isotropic Model presumes the vertical irradiance on the East and West sides of June to be smaller than the measurement value of 120 W/m$^2$ or more. The Perez Model agrees to the measurement values well, and is a good slope irradiance model, though the error becomes slightly large at no direct irradiance sky or turbid sky. The estimation values of the All Sky Model-R agrees to the measurement values very well regardless of the sky conditions, the season, the azimuth or the time of day. And the estimation method of the vertical irradiance based on the sky radiance distribution is proper.

The estimation values of the vertical illuminance by the All Sky Model-L are compared with the previous models and measurements. The CIE Standard General sky is not applied to this comparison since the selection range of the Types is wide. Examples of the comparison for the vertical illuminance between the calculated values by the All Sky Model-L, the All Weather Model of Perez et al. (1993) and the Isotropic Model, and the measurement values are shown in Fig. 17. The relation

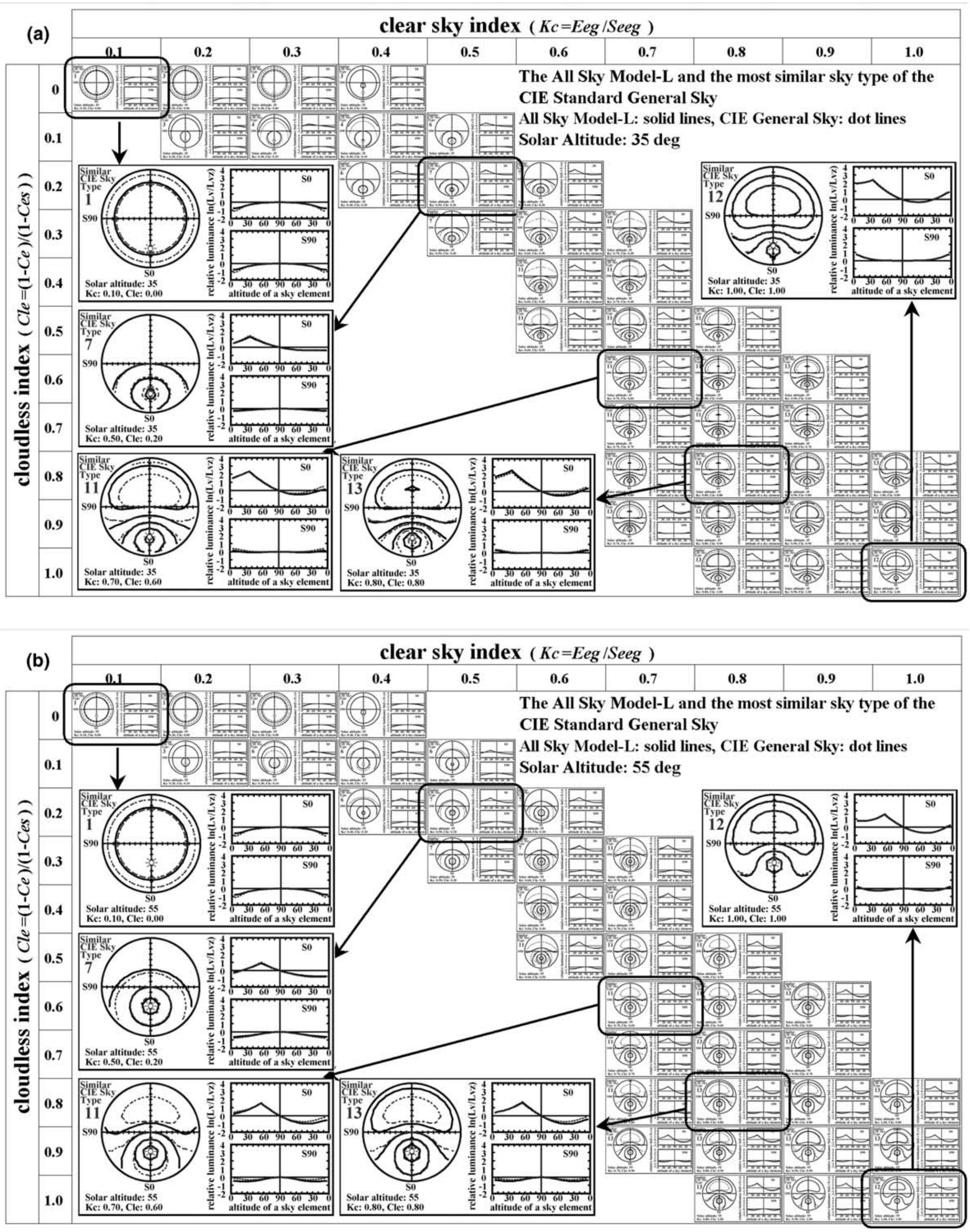


Fig. 15. The relative sky luminance distributions of the All Sky Mode-L and the most similar sky type of the CIE Standard General Sky.

between the estimation luminance and the measurement luminance indicates a tendency almost similar to the sky radiance distribution. The values estimated by the All Weather Model and the measurement values are

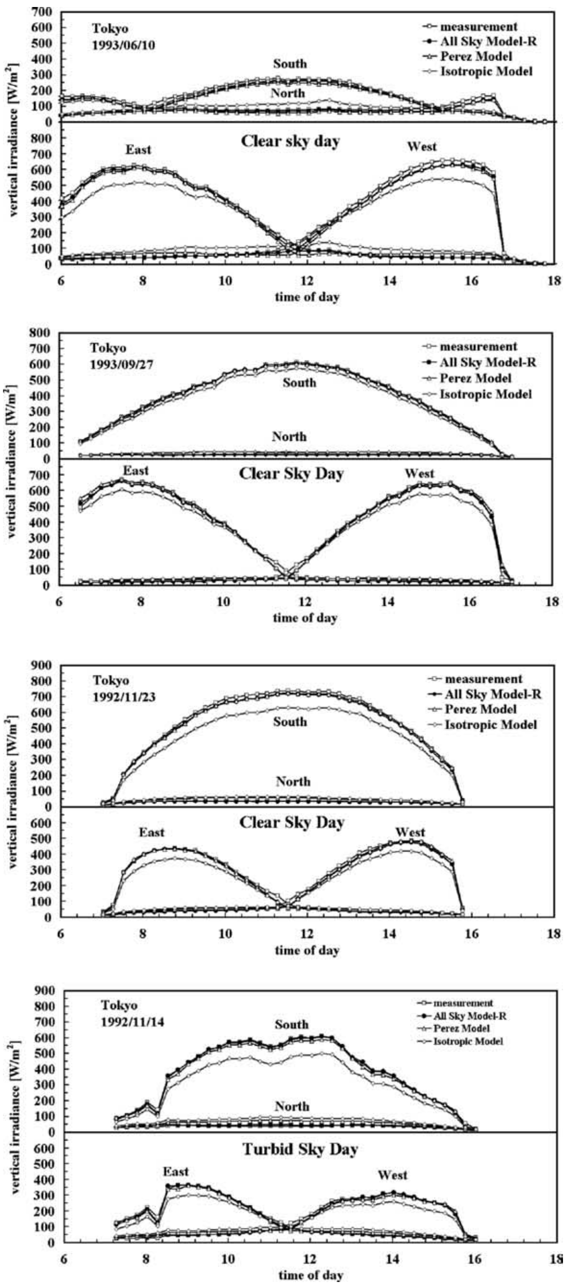


Fig. 16. Comparison of the vertical global irradiance between estimations and measurements.

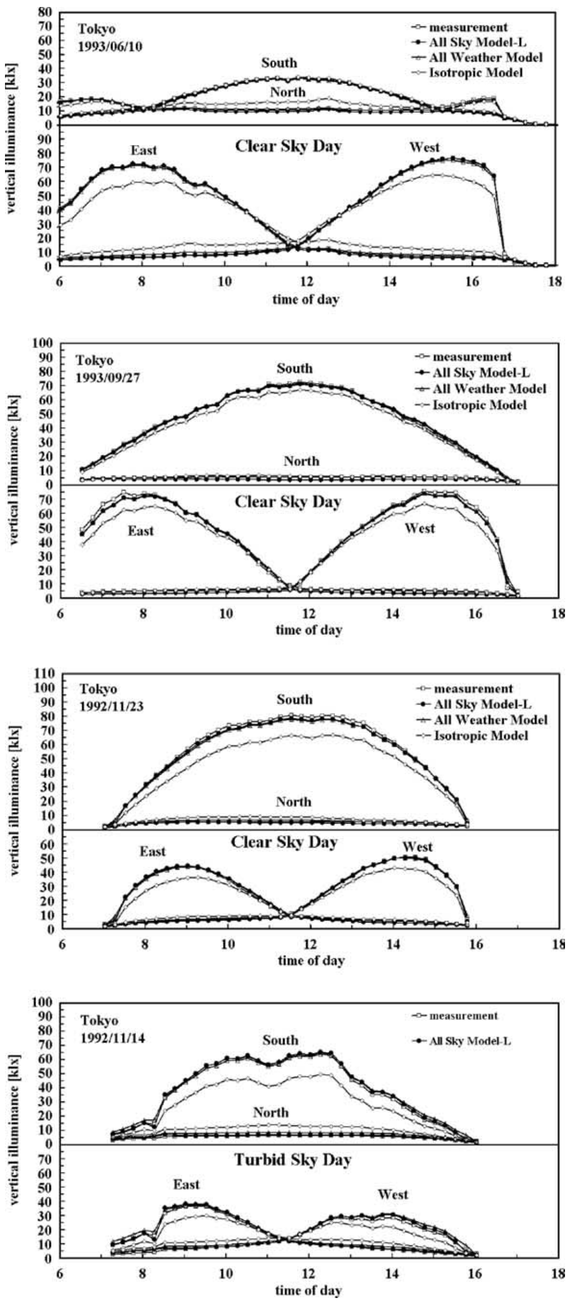


Fig. 17. Comparison of the vertical global illuminance between estimations and measurements.

resembled. Moreover, the estimation values of the All Sky Model-L are corresponding to the measurement values well.

The comparison of RMSE and MBE for the vertical irradiance is shown in Fig. 18. RMSE and MBE of the All Sky Model-R are smaller than those of the Perez Model for the irradiance. And the comparison of RMSE and MBE for the vertical illuminance is shown in Fig. 19. As for the daylight illuminance, RMSE and MBE of the All Sky Model-L are smaller than those of the All Weather Model. The Isotropic Model is greatly different from an actual phenomenon. The accuracies of the vertical irradiance by the All Sky Model-R and the vertical illuminance by the All Sky Model-L are considered to be practicably enough.

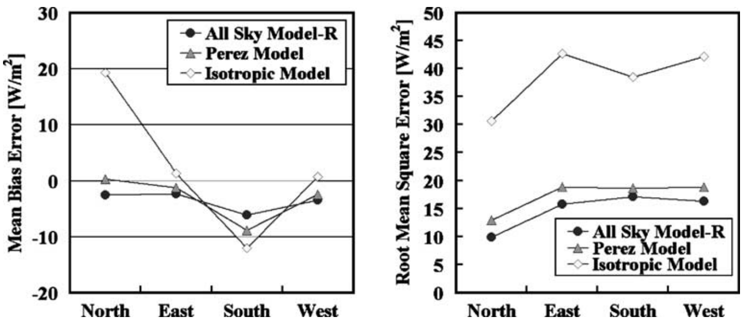


Fig. 18. MBE and RMSE of vertical irradiances.

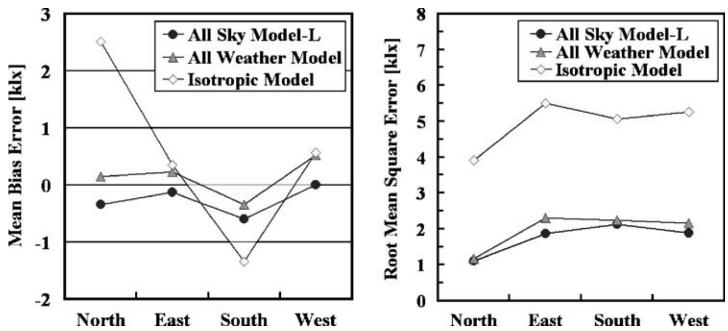


Fig. 19. MBE and RMSE of vertical illuminances.

## 6. Conclusions

The overall design technique that integrates the thermal environment and the luminous environment is necessary for the energy conservation and ensuring the quality of indoor environment. For the purpose, a minute, realistic model concerning the radiation and the daylight is required.

Ordinary, the daylight illuminance is not measured though the solar radiation is daily measured in the meteorological observatory. Therefore, it is reasonable to estimate sky conditions from the data concerning the solar radiation. That is, the method of classifying the sky condition proposed here is appropriate. In this paper, the method of classifying sky conditions from the solar radiation data was developed. And the equations to show sky radiance distribution and sky luminance distribution for all sky conditions called the All Sky Model-R and the All Sky Model-L were proposed.

Based on the All Sky Model-R and the All Sky Model-L, detailed meteorological data commonly used for the plan and design of thermal and daylight environment can be provided based on the global irradiance by the help of a suitable method of converting the global irradiance into the direct and diffuse irradiances and a suitable luminous efficacy model.

## References

Bird, R.E., 1984. A simple, solar spectral model for direct-normal and diffuse horizontal irradiance. Solar Energy 32 (4), 461–471.

Bourges, B., 1979. Reconstitution des courbes de fréquence cumulées de l'irradiance solarire globale horaire recue par une surface plane. Technical Report, Centre d'Engrgetique de l'Ecole Nationale Superieure des Mines de Paris.

Brunger, A.P., Hooper, F.C., 1993. Anisotropic sky radiance model based on narrow field of view measurements of shortwave radiance. Solar Energy 51 (1), 53–64.

CIE, 1955. Natural daylight, Official recommendation. Compte Rendu, CIE 13th Session, Committee E-3.2, vol. II, parts 3–2, II–IV&35–37.

CIE, 1973. Standardization of luminance distribution on clear skies. Pub. CIE No.22, TC-4.2.

CIE, 1994. Guide to recommended practice of daylight measurement. Pub. CIE 108, ISBN 3 900 734 50 X.

CIE, 2003. Spatial Distribution of Daylight—CIE Standard General Sky. Standard CIE S 011/E:2003.

Grant, R.H., Gao, W., Heisler, G.M., 1996. Photosynthetically active radiation: sky radiance distributions under clear and overcast conditions. Agric. Forest Meteorol. 82, 267–292.

Gueymard, C., 1989. A two-band model for the calculation of clear sky solar irradiance, illuminance, and photosynthetically active radiation at the earth's surface. Solar Energy 43 (5), 253–265.

Harrison, A.W., Coombes, C.A., 1988. An opaque cloud cover model of sky short wavelength radiance. Solar Energy 41, 387–392.

Harrison, A.W., 1991. Directional sky luminance versus cloud cover and solar position. Solar Energy 46 (1), 3–19.

Igawa, N., Nakamura, H., 2001. All Sky Model as a standard sky for the simulation of daylit environment. Build. Environ. 36 (6), 763–770.

Igawa, N., Nakamura, H., Matsuzawa, T., Koga, Y., Goto, K., Kojo, S., 1997. Sky luminance distribution between two CIE Standard Skies (Part 2) Numerical equation for relative sky luminance distributions. in: Proceeding of the 3rd LUX PACIFICA, Nagoya, pp. E13–E18.

Igawa, N., Nakamura, H., Koga, Y., Matsuzawa, T., Yoshimura, K., 2002. Development of a sky radiance distribution model for all sky conditions. In: Proceedings of the 3rd European Conference on Energy Performance and Indoor Climate in Buildings, Lyon, pp. 643–648.

Japan Meteorological Agency, 1995–2001, Annual Report.

Kasten, F., 1984. Parametrisierung der Globalstahlung durch Bedeckungsgrad und Trubungsfaktor. Ann. Meteorol. Neue Folge 20, 49–50.

Kasten, F., Young, A.T., 1989. Revised optical air mass tables and approximation formula. Appl. Opt. 28 (22), 4735–4738.

Kittler, R., 1967. Standardization of outdoor conditions for the calculation of daylight factor with clear skies. In: Proceedings of the CIE International Conference on Sunlight in Buildings, Bouwcentrum International, Rotterdam, pp. 273–285.

Kittler, R., 1985. Luminance distribution characteristics of homogeneous skies: a measurement and prediction strategy. Light. Res. Technol. 17 (4), 183–188.

Kittler, R., 1986. Luminance Models of Homogeneous Skies for Design and Energy Performance Predictions. In: Proceedings of the 1st, 1986 International Daylighting Conference, Long Beach, pp. 18–22.

Kittler, R., Perez, R., Darula, S., 1997. A new generation of sky standards. In: Proceedings of the Lux Europa '97, pp. 359–373.

Kondo, J., 2000. Atmospheric science near the ground surface. University of Tokyo Press, ISBN-13-062707-4 (in Japanese).

Littlefair, P.J., 1981. The luminance distribution of an AVERAGE SKY. Light. Res. Technol. 13 (4), 192–198.

Matsuzawa, T., Nakamura, H., Igawa, N., Koga, Y., Goto, K., Kojo, S., 1997. Sky luminance distribution between two CIE Standard Skies (Part 1) Arrangement of the sky luminance distribution data measured. In: Proceedings of the 3rd LUX PACIFICA, Nagoya, pp. E7–E12.

Moon, P., Spencer, D.E., 1942. Illumination from a non-uniform sky. Trans. Illum. Engng. Soc. 37, 707–726.

Nagata, T., 1997. Radiance distribution on stable overcast skies. J. Light Vis. 21 (1), 6–9.

Nakamura, H., Oki, M., Hayashi, Y., 1985. Luminance distribution of intermediate sky. J. Light Vis. Env. 9 (1), 6–13.

Nakamura, H., Oki, M., Iwata, T., 1987. Mathematical description of the intermediate sky. In: Proceedings of the 21st CIE Session, Venice, vol. 1, pp. 230–231.

Nakamura, H., Oki, M., Koga, Y., 1991. New sky scanner for the measurement of sky luminance distribution. Proceedings of the 22nd Session of the CIE 1(1), Melbourne, pp. 61–62.

Nakamura, H., Kojo, S., Koga, Y., Seo, J., Igawa, N., Anai, K., 1997a. A study on sky radiance distribution. Part 1. Relative sky radiance distribution by solar altitude. J. Illum. Engng. Inst. Jpn. 81 (2), 26–36 (in Japanese).

Nakamura, H., Kojo, S., Koga, Y., Seo, J., Igawa, N., Anai, K., 1997b. A study on sky radiance distribution. Part 2. Equation for the relative yearly average mean sky radiance distribution. J. Illum. Engng. Inst. Jpn. 81 (2), 110–120 (in Japanese).

Nakamura, H., Kojo, S., Koga, Y., Seo, J., Igawa, N., Anai, K., 1997c. A study on sky radiance distribution. Part 3. Equation for the zenith radiance and the absolute yearly a mean sky radiance distribution. J. Illum. Engng. Inst. Jpn. 81 (5), 12–20 (in Japanese).

Perez, R., Ineichen, P., Seals, R., Michalsky, J., Stewart, R., 1990. Modeling daylight availability and irradiance components from direct and global irradiance. Solar Energy 44 (5), 271–289.

Perez, R., Seals, R., Michalsky, J., 1993. All-weather model for sky luminance distribution—preliminary configuration and validation. Solar Energy 50 (3), 235–245.

Perraudeau, M., 1988. Luminance models. National Lighting Conference 1988, Cambridge, pp. 291–292.

Rigollir, C., Bayer, O., Wald, L., 2000. On the clear sky model of ESRA—European solar radiation atlas—with respect to the heliosat method. Solar Energy 68 (1), 33–48.

Yang, K., Huang, G.W., Tamai, N., 2001. A hybrid model for estimating global solar radiation. Solar Energy 70 (1), 13–22.